THREE DIMENSIONAL TRANSONIC FULL POTENTIAL SOLUTION BY AN INTEGRAL EQUATION METHOD

N.L. Arora* and J.P. Agarwal**
Department of Aerospace Engineering
Indian Institute of Technology, Kanpur, INDIA

Abstract

A computational scheme based on integral equation approach for the solution of full potential equation (FPE) for steady inviscid transonic flow over three dimensional configurations, has been developed. Application of Green's third identity to the FPE yields an integral equation for the disturbance potential, in terms of surface source and doublet distribution, and nonlinear field source distribution representing compressibility. The solution thus constructed automatically satisfies the boundary condition at infinity. The problem is discretized by surface panels in conjunction with the field cells, formed by rectangular box of grid points around the configuration. The surface panels are used to enforce the boundary condition on the body surface and the field cells are used to evaluate the volume integral. The surface source distribution is determined by the external Neumann boundary condition. The Kutta condition is imposed for the determination of the doublet distribution, the values of the surface velocity potential. This gives rise to an iterative procedure for the numerical solution of the integral equation. For supercritical flow with shocks an artificial viscosity is added explicitly to produce upwind bias at supersonic points which enables shock capture. Results are obtained for the pressure distribution on finite wings.

I. Introduction

Although a great deal of progress has been made in solving nonlinear fluid flow problems by finite difference methods, these methods have not yet proved to be easily adaptable to complex three dimensional surfaces. Probably the major obstacle in computing inviscid transonic flow about complete aircraft is the difficulty of generating `body conforming' grids.

Recently computational schemes have been developed based on integral equation (IE) formulation[1-10] for solving the full potential equation (FPE) for steady inviscid transonic flow, which obviates the need for body conforming grids. The concept of zonal modelling, in which a field metod is coupled with a surface panel method, as used in these studies looks attractive for extending the practical scope of surface panel methods into transonic regime, via the field integrals.

In the present work a hybrid computational scheme is developed for the analysis of transonic flow over three dimensional configurations, which is based on the integral eqation formulation and makes use of the elements from the finite difference methods.

Application of Green's third identity to the FPE, for subsonic free stream values, yields an integral equation for disturbance velocity potential in terms of surface source and doublet singularity distributions, and the nonlinear field source distribution representing compressibility. The solution thus constructed automatically satisfies the boundary condition at infinity. Since the field sources die rapidly away from the body, only a small computational domain around the body would then suffice to solve the flow problem.

To obtain numerical solution of the integral equation, surface panels are used in conjunction with the field volume elements. The configuration surface and the wake is represented by a number of flat quadrilateral panels and the singularity distribution is assumed piecewise constant over each panel. A rectangular three dimensional grid is generated within a finite volume around the configuration and the wake, which encompasses and penetrates the body. The cells formed by the rectangular grid are used as finite elements, wherein the field source strengths are assumed to be uniform. Thus the field grid is independent of the surface geometry, and the entire problem of generating a surface conforming grid, a major obstacle in solving the transonic flow problem by the finite difference methods, is avoided.

The surface panels are used to enforce the boundary condition on the body surface and the field cells are used to evaluate the volume integral. The surface source distribution is determined by the external

* Professor, ** Research Engineer

Neumann boundary condition and the Kutta condition is enforced for the determination of the doublet distribution, the values of the surface velocity potential, unknown of the flow problem. Application of the Kutta condition is simple, and no extra equation or trailing edge velocity potential is required.

This gives rise to a Poisson type iterative procedure for the numerical solution of the integral equation. To obtain the surface velocity and hence the pressure distribution, the surface potentials are differentiated numerically.

For supercritical flow with shocks the nonlinear source term is augmented by the addition of artificial viscosity in the supersonic region which produces an upwind bias and satisfies the proper domain of dependence. A mass flux biasing (instead of the usual density biasing, e.g. Ref. 11 & 12) is used for modelling the artificial viscosity following Osher, Hafez and Whitlow[13].

First the general formulation of the integral equation for the FPE, which is similar to the one given by Erickson and Strande[4], is presented. This is followed by the derivation of the integral equation for the present model, discretization of the flow problem, evaluation of the influence coefficients, formulation of the artificial viscosity, and finally the iterative scheme for the solution of nonlinear transonic flow is set up. The present method differs from that of Sinclair[5] in the sense that Sinclair uses velocity formulation, whereas our method is based on velocity potential formulation. Thus the present method requires much less storage and computation of smaller number of influence coefficients, and hence low computing cost. This makes it more suitable for application to complex configurations at transonic speeds.

As examples of computation, we have considered RAE Wing C and ONERA M-6 wing. The results are obtained for nonlinear flow at high subsonic free stream Mach numbers - subcritical, shock free supercritical, and supercritical flow with shocks, and compared with the well established results.

The simplicity of piecewise constant singularity panels offers great flexibility for application to complex configurations; since continuity of singularity distribution is not enforced from panel to panel, the assembly of panels representing a complicated surface is fairly straight forward. Further the low computing cost of this method makes it attractive for applications to nonlinear flow problems requiring iterative solution.

The major advantage of the computational scheme attempted here is its inherent capability to treat the complex configurations with the same ease as a simple 3-D wing, which otherwise would require an elaborate body conforming grid generation, a formidable task in itself.

II. Formulation

The full potential equation for steady inviscid compressible flow past three-dimensional aerodynamic configuration can be expressed as

$$\nabla^2\phi(x,y,z) = -\frac{1}{\rho}(\nabla\rho.\nabla\phi) \qquad (1)$$

where

$$\rho = [1 + \tfrac{1}{2}(\gamma - 1)\, M_\infty^2\, (1 - \nabla\phi.\nabla\phi)]^{1/(\gamma-1)}$$

Subscript ∞ refers to the undisturbed free stream conditions. The velocity $q = \nabla\phi$ and density ρ have been normalized by their free stream values. Reading Eq.(1) as Poisson's equation, the application of Green's third identity yields for the perturbation potential at the point P(x,y,z) in the field as

$$\varphi = \iint_S (\sigma K_\sigma + \mu K_\mu)\, dS + \iiint_D G\, K_\sigma\, dV \qquad (2)$$

where $\varphi = \phi - \phi_\infty$

$$K_\sigma = -1/(4\pi R), \quad K_\mu = \hat{n}.\nabla_Q\{-K_\sigma\}$$

$$\vec{R} = \vec{Q} - \vec{P} \equiv (\xi - x,\ \eta - y,\ \zeta - z)$$

$$\sigma = \Delta(\partial\varphi/\partial n), \quad \mu = \Delta\varphi$$

and $G = (-1/\rho)\,(\nabla\rho.\nabla\phi)$

Here Δ represents jump across the surface S that bounds D and D', see Fig. 1;

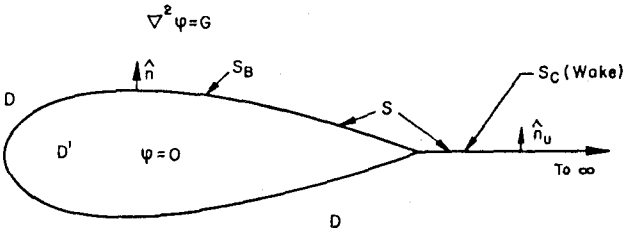

Figure 1. Fluid Domain and Boundary

In the surface integral Q, Eq. (2) represents a variable point of surface S, whereas in the volume integral Q represents a variable point of domain D;

R is the distance from the field point P to the variable point Q;

$\hat{n}.\nabla_Q = \partial/\partial n$ represents the derivative normal to the surface S, directed into domain D.

Equation (2) states that the velocity potential at a particular point P can be computed from the source and doublet distribution on S (taken to be the configuration surface and the wake), and from the spatial distribution of G, representing the compressibility in the domain D around S.

Since G in Eq.(1) is a nonlinear function of φ, $\varphi(P)$ cannot be constructed directly, as is done with the solution of the linear equation

$$\nabla^2\varphi = 0$$

which is represented by

$$\varphi(P) = \iint_S (\sigma K_\sigma + \mu K_\mu)\, dS$$

Thus distributrion of $\varphi(x,y,z)$ that satisfies Eq. (2) and the boundary conditions on S, must be determined by some iterative procedure. If this is done, it follows from Eq. (1) that

$$\iiint_D (\nabla^2\varphi - G)\, K_\sigma\, dV = 0$$

i.e. the full potential equation has been satisfied throughout D.

Boundary Conditions

The boundary condition at infinity is automatically satisfied by Eq. (2).

On the body surface, the total normal component of velocity must vanish,i.e.

$$\hat{n}.\nabla\phi = 0 \qquad (3)$$

Setting the perturbation potential in the interior of the surface S to zero, i.e.

$$\varphi = 0 \quad \text{in } D' \qquad (4)$$

the interior Dirichlet boundary condition, the source distribution on the body surface becomes $\sigma = \partial\varphi/\partial n$, and the doublet distribution $\mu = \varphi$, the perturbation potential on the body surface.

Then using (3), the source distribution on S is determined, a priori, as

$$\sigma = -\hat{n}.\nabla\phi_\infty \qquad (5)$$

In addition, the Kutta condition is specified at the trailing edge.

Integral Equation

With source strength σ specified through Eq. (5), Eq. (2) gives for the potential at the field point P

$$\begin{aligned} E^*\varphi(P) = &\iint_{S_B} \sigma(Q)\, K_\sigma\, dS \\ &+ \iint_{S_{B-P}} \phi(Q)\, \hat{n}.\nabla_Q(-K_\sigma)\, dS \\ &+ \iint_{S_C} \Delta\varphi_W(Q)\, \hat{n}_u.\nabla_Q(-K_\sigma)\, dS \\ &+ \iiint_D G(Q)\, K_\sigma\, dS \end{aligned} \qquad (6)$$

with $E^* = 1/2$, for points on the body surface
$= 1$, for points in the domain D

and $\varphi = 0$, for points inside the body, domain D'.

Here S_B and S_C indicate the body and the wake surfaces respectively; S_{B-P} indicates that S_B does not contain point P;
$\Delta\varphi_W = \varphi_u - \varphi_l$ represents the difference in potential across S_C and $\hat{n}_u$ represents the unit outward normal drawn to the upper surface of S_C. Moreover $\Delta(\hat{n}_u.\nabla\varphi) = 0$ on S_C, which is assumed to lie in the x-y plane.

Also note that $\Delta\varphi_W$ is constant in the wake along a streamline and equals to the value at the trailing edge (te), at any spanwise location, i.e.

$$\Delta\varphi_W = \Delta\varphi_{te},$$

since no pressure difference can exist across the wake.

III. Numerical Solution

Discretization

For the numerical solution of integral equation (6), the body surface and the wake is represented by a number of flat quadrilateral panels , see Fig. 2, and a constant singularity distribution is assumed on each panel.

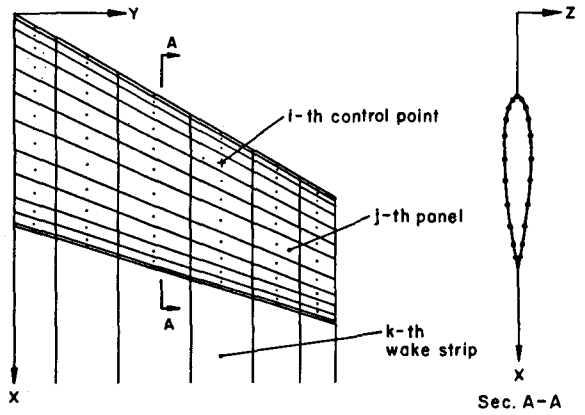

Figure 2. Surface Panelling

Although D is the complete domain external to the configuration, the field source strengths G decay rapidly away from the surface, and so in practice only a limited region around the configuration would be sufficient to solve the flow problem. Therefore a region of space including the configuration and its immediate neighbourhood is subdivided into finite volume cells with Cartesian grid, which penetrates the configuration, Fig.3. The field source strengths are assumed to be uniform in each cell.

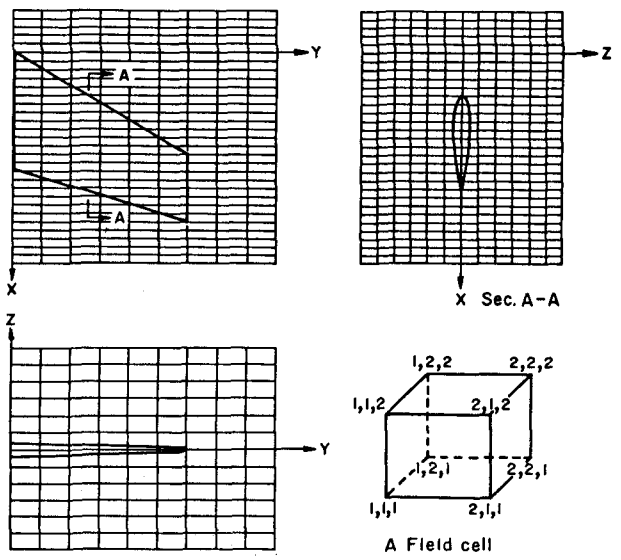

Figure 3. Field Grid

Thus we have the standard surface panelling along with the field grid, and two set of control points. The surface control points are taken to be the centroids of the surface panels, where the surface sources are specified and thus the Neumann condition is imposed. The field control points are defined as the centroids of the cells, where the field source distributions are evaluated.

Assigning index i to each control point at which Eq.(6) is to be satisfied, we obtain,

$$E^{*}\,\varphi_i = \sum_{j=1}^{Ns} \sigma_j\, B_{ij} + \sum_{\substack{j=1 \\ i\neq j}}^{Ns} \varphi_j\, C_{ij} + \sum_{k=1}^{Nw} (\Delta\varphi)_k\, Cw_{ik} + \sum_{n=1}^{Ng} G_n\, D_{in} \qquad (7)$$

where $E^{*} = 1/2$, for i = 1,2 ... Ns, surface control points (CP)
$= 1$, for i = 1,2 ... Ng, field points (GP)

Ns is the total number of surface panels on the body, Nw is the total number of streamwise wake columns, and Ng is the total number of field cells.

$$\Delta\varphi = \varphi_{Nu} - \varphi_{Nl}$$

$$B_{ij} = \iint_{\Sigma_j} K_\sigma \, dS, \qquad C_{ij} = \iint_{\Sigma_j} \hat{n}.\nabla_a(-K_\sigma)\, dS$$

$$Cw_{ik} = \iint_{\Sigma_k} \hat{n}_u.\nabla_a(-K_\sigma)\, dS$$

$$D_{in} = \iiint_{\Delta V_n} K_\sigma \, d\xi \, d\eta \, d\zeta$$

φ_{Nu} and φ_{Nl} are taken as the values of the potential on the panels adjacent to the trailing edge at the start of the k-th wake column.

B_{ij} and C_{ij} represent the potentials induced at the i-th control point due to a source and a doublet distribution of unit strength respectively on the j-th surface panel.

D_{in} is the potential induced at the i-th control point due to a uniform unit source distribution in the n-th field cell.

The surface integrations are indicated on flat quadrilateral j-th panel Σ_j, and k-th wake column Σ_k, and volume integration on n-th field cell ΔV_n.

Equation (7) with $G_n = 0$ gives rise to a low order surface panel method for incompressible flow problem. This approach has been pioneered by Morino[14], and forms a subset of general method of Johnson[15] for incompressible flows.

Evaluation of Influence Coefficients

The surface influence coefficients B_{ij} C_{ij} and Cw_{ik} can be easily evaluated, following Johnson[15] in the panel coordinate system attached with the influencing panel j. The summations indicated over the body surface and the wake in Eq. (7) are then straightforward, as no further coordinate transformation is required.

The field source influence coefficient for each of the field cells, external to the body in domain D, can be evaluated analytically in terms of the grid points forming the cell. The resulting expressions are presented in the appendix. It may be observed that the identical field cells (n = 1,2,..Ng) with their centroids located at the same axiswise distance from the field control point i will have the same value of D_{in}. This symmetry property is exploited in the evaluation of D_{in}, which reduces the number of calculations considerably, and more important a saving in the overall storage can be achieved.

The body surface slices through some of the field cells, which alters the finite volume discretization in the vicinity of the boundary surface. An exact evaluation of field source integrals for such cells, which are of trapezoidal shape, can be easily achieved by the use of divergence theorem of Gauss. It can be shown that the field integral for such a cell is the same as the field integral over the complete cuboid which partly lies inside the body, i.e. domain D', with the source strength evaluated on the body surface from the external field.

Since $\varphi(P) = 0$ inside the domain D', the value of the volume integral over the cells completely lying inside the body will be zero.

The evaluation of the field integral is thus a simple summation for all the field sources.

Construction of Artificial Viscosity

The full potential equation in conservative form is written as

$$\nabla.(\rho \underline{q}) = 0 \qquad (8)$$

with $\underline{q} = \nabla\phi$. In the finite difference schemes, the central difference approximation for this equation is unable to capture shocks for supercritical flows, as it mimics the behaviour of an elliptic system. In supercritical flows, the hyperbolicity of the equation should be ensured at supersonic points. To simulate this, upwind differencing is accomplished by the addition of artificial viscosity $\underline{A}(P,Q,R)$. Equation (8) can then be written in conservative form as

$$\nabla.(\rho \underline{q} + \underline{A}) = 0 \qquad (9)$$

The term $\underline{A}$ has been modelled in the literature in various forms for density biasing schemes (see e.g. Ref 11 and 12), which differ slightly in details giving almost similar results.

Here we consider modelling the artificial viscosity following Osher, Hafez and Whitlow[13], referred to as Hafez-Osher (H-O) scheme. This scheme uses upwinding of the mass flux rather than the density, and yields the following form for the derivatives of the artificial viscosity

$$\frac{\partial P}{\partial x} = -\Delta x \overrightarrow{\delta}_x\left[\frac{(\overleftarrow{\delta}_x\phi)^+}{q}\overleftarrow{\delta}_x(\rho q)_-\right], \quad \overleftarrow{\delta}_x\phi > 0$$

$$= \Delta x \overleftarrow{\delta}_x\left[\frac{(\overrightarrow{\delta}_x\phi)^-}{q}\overrightarrow{\delta}_x(\rho q)_-\right], \quad \overrightarrow{\delta}_x\phi < 0 \qquad (10)$$

where $\overleftarrow{\delta}_x$ and $\overrightarrow{\delta}_x$ refer to backward and forward differencing respectively, and the operations

$$g^+ = \max(g,0), \quad g^- = \min(g,0)$$

The term $(\rho q)_-$ is expressed as

$$(\rho q)_- = \rho q - \rho^* q^*, \quad \text{if } q > q^* \iff M > 1,$$

$$(\rho q)_- = 0, \quad q \le q^* \iff M \le 1$$

The quantities ρ^* and q^* represent the sonic condition given by

$$(q^*)^2 = \frac{2 + (\gamma-1) M_\infty^2}{(\gamma+1) M_\infty^2}$$

$$\rho^* = (q^* M_\infty)^{2/(\gamma-1)}$$

On discretization, Eq. (12) gives

$$\left(\frac{\partial P}{\partial x}\right)_i = -\frac{1}{q_{i+1}}(UD)_{i+1/2} + \frac{1}{q_i}(UD)_{i-1/2}, \quad u_{i-1/2} > 0$$

$$= \frac{1}{q_i}(UD)_{i+1/2} - \frac{1}{q_{i-1}}(UD)_{i-1/2}, \quad u_{i+1/2} < 0 \qquad (11)$$

where

$$(UD)_{i+1/2} = \frac{(\rho_{i+1}q_{i+1})_- - (\rho_i q_i)_-}{x_{i+1} - x_i} u_{i+1/2}$$

and $u = \phi_x$

Similar expressions are obtained for $\partial Q/\partial y$ and $\partial R/\partial z$.

The H-O scheme admits physically correct limit solutions to the FPE, and hence more appropriate to model the artificial viscosity. The other advantage of this scheme is that there is no need for the user defined parameters to control the artificial dissipation, as are usually required for the density biasing schemes[11].

Iteration Scheme

The construction given by Eq. (7) is turned into an iterative procedure. The iteration starts with an initial guess of G_n. The simplest choice would be $G_n^\circ = 0$. Equation (7) then corresponds to the solution of Prandtl Glauert equation, and gives Ns linear algebraic eqations for the values of φ at the surface control points i= 1,2...Ns, i.e. $\{\varphi^\circ(CP)\}$

With the surface values of $\{\varphi^\circ(CP)\}$ known and the initial guess of G_n°, compute $\{\varphi^\circ(GP)\}$ at the field cells centroids, using Eq. (7). The gradients of the potential, the density and its gradients are then computed in the field by finite differences, to provide the first estimate of G_n^1 over all the field cells. Finally the field integral f(P) is computed as

$$f^1(P) = \sum_{n=1}^{Ng} G_n D_{in} \qquad (12)$$

With $\{f^1(CP)\}$ known, Eq. (7) is again solved for $\{\varphi^1(CP)\}$ as solution of Ns linear algebraic equations for the surface control points.

Thus $\varphi^m(CP)$ at the mth iteration is obtained by the following steps:

$$\varphi^{m-1}(GP) = fn\{\varphi^{m-1}(CP), f^{m-1}(P)\} \qquad (13a)$$

$$G_n^m = fn\{\varphi^{m-1}(GP)\} \qquad (13b)$$

$$f^m(P) = \sum_{n=1}^{Ng} G_n D_{in} \qquad (13c)$$

Solve Eq.(7) for $\varphi^m(CP)$ using $\varphi^{m-1}(CP)$ and $f^m(GP)$ (13d)

The iteration cycle is continued till $\varphi(CP)$ converges.

During every iteration we are led to a set of Ns linear algebraic eqations, which are solved by the Gauss-Siedel iterative procedure with successive over-relaxation, providing Ns disturbance potential on the body surface. The over-relaxation factor is optimized by numerical experimentation.

To accelerate the convergence for supercritical cases, one more step may be introduced in the above cycle, i.e. modify $\varphi^{m-1}(GP)$ as obtained from step (13a), before it is made use of in step (13b), as follows

$$(\varphi)^{m-1}(GP) = \lambda\varphi^{m-1}(GP) + (1-\lambda)\varphi^{m-2}(GP) \qquad (14)$$

where $(\varphi)^{m-1}$ represents the modified value of φ^{m-1} at (m-1)th iteration.

A good choice of λ reduces the number of iterations considerably. In the present computations the following choice of λ was made

$$\lambda = 0.5, \quad M \geq 1.5$$

$$= 2 - M, \quad 1.5 > M \geq 1$$

$$= 1 + (1-M^2)^{1/2}, \quad 0 \leq M < 1$$

where M is the local Mach number. This choice reduces the number of iterations by about one third.

The iterative solution yields the Ns disturbance potential on the body surface. A local linear distribution of φ is then assumed using values at five panel centres, that is a central panel and its four immediate neighbours. The surface potentials are differentiated using the least square procedure. This together with the tangential component of free stream velocity provides the local total velocity on the wing surface,

$$q = |\hat{e}_\infty + \nabla\varphi| \qquad (15)$$

$\hat{e}_\infty$ being the unit vector in the direction of the free stream.

The pressure is finally computed using the isentropic relation

$$C_p = \frac{2}{\gamma M_\infty^2}\left[\left\{1 + \frac{\gamma-1}{2} M_\infty^2(1-q^2)\right\}^{\frac{\gamma}{\gamma-1}} - 1\right] \quad (16)$$

IV. Results and Discussion

The pressures are computed on ONERA M-6 wing for subcritical onflow at free stream Mach number of 0.5 at an incidence of 3° using 62 x 9 surface panels, 9 wake strips and 40 x 12 x 20 field cells. The results at spanwise location η (= y/semi-span) = 0.4313 are presented in Fig. 4, and compared with an Euler solution of Salmond[16], which uses 129 x 17 x 41 grids. A good agreement is indicated considering relatively small number of field cells in the present computation.

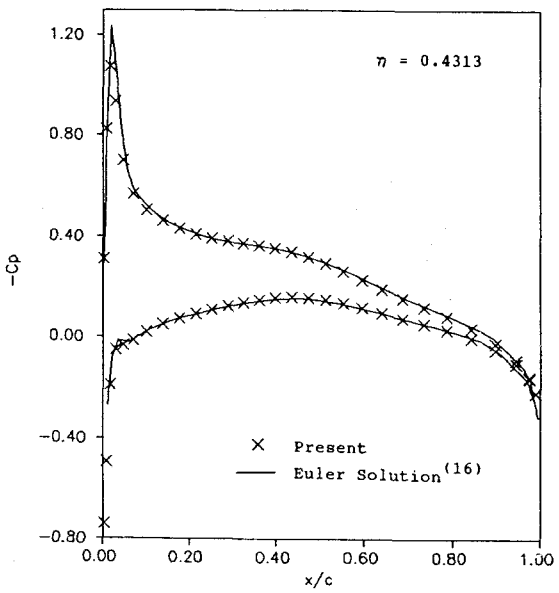

Figure 4. Pressure Distribution Comparison ONERA M-6 Wing: $M_\infty = 0.5$, $\alpha = 3^\circ$

Next we have considered RAE wing C, t/c = 0.054 at $M_\infty = 0.95$, $\alpha = 0^\circ$, a non-lifting supercritical shock free case. The results are obtained with 56 x 9 surface panels and 40 x 12 x 20 field cells. A comparison is made with RAE test data and finite difference TSP solution of Bailey and Ballhaus[17], Fig. 5. A good agreement is indicated in this case, however at η = 0.75, our results show a slightly enlarged supersonic zone and the onset of shock is perceptible.

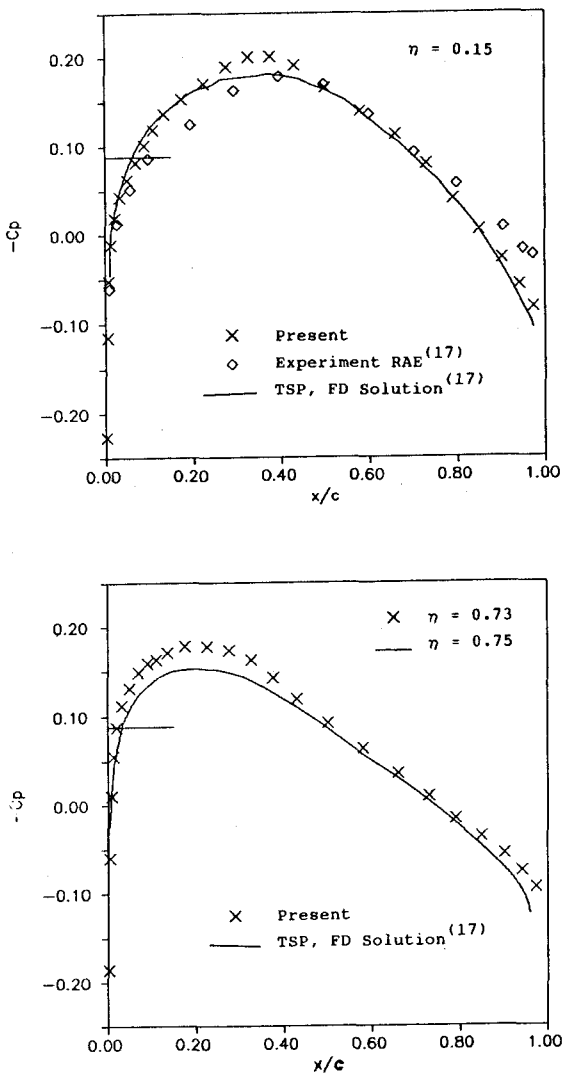

Figure 5. Pressure Distribution Comparisons RAE Wing C: t/c = 0.054 at $M_\infty = 0.95$, $\alpha = 0^\circ$

Finally, we have considered M-6 wing at $M_\infty = 0.84$ and $\alpha = 3.06^\circ$, a supercritical case with shocks.

The right half of the wing is defined with 62 x 9 surface panels, 9 wake strips and 40 x 12 x 20 field cells around the wing in the x, y and z directions respectively, in a rectangular box bounded by

$-0.125 \le x/c \le 1.539$, $0 \le \eta \le 1.333$ and

$-2.60 \le z/c \le 2.60$,

with c as the root chord.

The field grid spacing along the x and y directions is chosen uniform with Δx and Δy different, whereas a stretched grid spacing is employed in the z direction. The results for the pressure distribution are presented in Fig. 6.

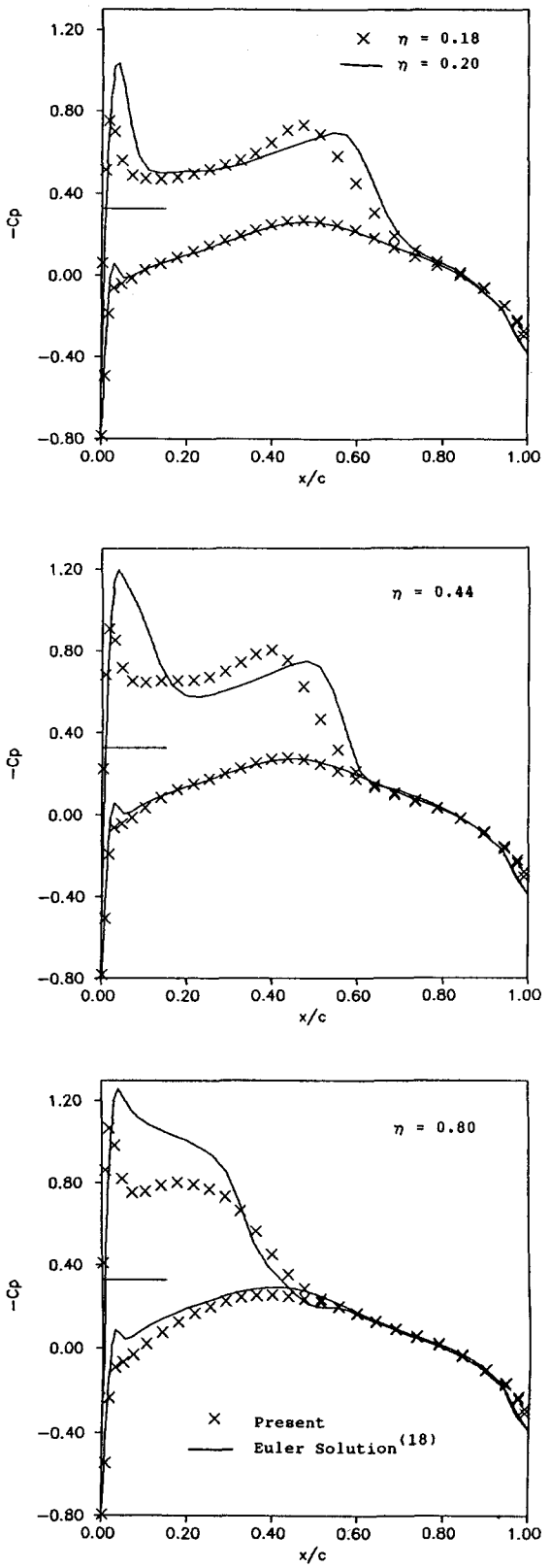

Figure 6. Pressure Distribution Comparisons ONERA M-6 Wing: $M_\infty = 0.84$, $\alpha = 3.06^\circ$

They are compared with the AGARD test cases[18], which are solutions of Euler equations based on a very fine grid extending to large boundaries around the wing.

The computed results at the spanwise location $\eta = 0.18$ look very promising. The shock location is predicted well, however it is smeared over 5-6 field cells. Also near the leading edge, the pressure peaks are not resolved fully. The results seem to deteriorate as one moves away from the root towards the tip. The number of field cells along the wing chord in the x-direction at $\eta = 0.18$, 0.44 and 0.80 are 22, 19 and 15 respectively, yielding $\Delta x/c$= 0.0452, 0.0515 and 0.064 at these locations. These values of Δx are obviously too coarse to either give a sharp shock or to resolve the pressure peaks near the leading edge adequately. This observation is in accord with the trends reported in the TRANAIR[6,7] results. Further it may be noted that the computational domain considered extends only 0.125c ahead of the wing at the root chord which is quite inadequate. Also no effort was made to model the wing tip. Limited experimentation has shown that increasing the field cell density in the x-direction reduces the smearing of the shock and shows improvement in the overall results including the outboard stations. Further experiments and improvement are currently at hand.

The above set of three computations took 4, 10 and 28 iterations respectively to achieve a residual error of 0.0002 in each of the above computations. The overall grid size was dictated by the computational resources of the HP-9000 system available at IIT Kanpur.

V. Concluding Remarks

The computational scheme presented, based on IE method, is capable of treating steady transonic flow past three dimensional configurations, for subsonic free stream speeds, successfully. The formulation is of shock capturing type and the contribution of shock, as a source of disturbance, is embedded in the volume integral term. To obtain good flow resolution, a finer computational grid forming the field cells would be needed in the regions of rapidly varying flow, e.g. shock regions and pressure peaks.

The IE method has several advantages in comparison with the finite difference (FD) solution. With the IE formulation the far field boundary condition is automatically satisfied, and only a small computational domain is needed around the source of disturbance. The accuracy of the method depends on the evaluation of integrals rather than the derivatives, and hence coarse grids can be adopted.

The computational scheme developed appears efficient in terms of the overall iteration count as compared with the other existing schemes that use finite difference/finite volume methods throughout large computational domain with fine grid. However the major advantage of the scheme attempted here is its inherent capability to treat the complex configurations with the same ease as a simple 3-D wing, which would otherwise require an elaborate procedure for body conforming grid generation, a formidable task in itself.

Further improvements/refinements of the method and its extension to complex configurations are currently being taken up.

Appendix

Field Source Influence Coefficients

The field source influence coefficient D_{in} in terms of the Cartesian grid points forming the field cell ΔV_n is given by,

$$D_{in} = \int_{\xi_1}^{\xi_2}\int_{\eta_1}^{\eta_2}\int_{\zeta_1}^{\zeta_2} \frac{-1}{4\pi R}\, d\xi\, d\eta\, d\zeta \qquad (A1)$$

Here the integration is indicated over the grid points (vertices) of the field cells, and

$$R = [(\xi-x)^2 + (\eta-y)^2 + (\zeta-z)^2]^{1/2}$$

The volume integral

$$I = \iiint (-1/R)\, d\xi\, d\eta\, d\zeta$$

can be evaluated analytically to yield,

$$\begin{aligned} I = {} & AB \ln\{(H+C)/D\} + AC \ln\{(H+B)/E\} \\ & + BC \ln\{(H+A)/F\} \\ & + \tfrac{1}{2}[B^2 \tan^{-1}\{BH/(AC)\} \\ & + C^2 \tan^{-1}\{CH/(AE)\} + A^2 \tan^{-1}\{AH/(BC)\}] \end{aligned} \qquad (A2)$$

with $A = x - \xi$, $B = y - \eta$, $C = z - \zeta$,

$D^2 = A^2 + B^2$, $E^2 = A^2 + C^2$, $F^2 = B^2 + C^2$,

and $H^2 = A^2 + B^2 + C^2$.

Integral I is evaluated at all the vertices of the field cell, see Fig. 3, to obtain the influence coefficient D_{in}. Thus

$$\begin{aligned} D_{in} = 1/(4\pi)\, [& I(2,2,2) + I(1,1,2) \\ & + I(1,2,1) + I(2,1,1) \\ & - I(1,2,2) - I(2,1,2) \\ & - I(2,2,1) - I(1,1,1)] \end{aligned} \qquad (A3)$$

The computations of field source coefficients is most time consuming. However, about 90% of the field source coefficients may be computed by using the far field approximation as follows, which results in considerable efficiency.

Far Field Approximation

For the field cells far away from the field control point, the uniform source distribution in the field cell may be replaced by a point source at its centroid. In that case

$$D_{in} = -1/(4\pi R_{in})\, \{DV_n\} \qquad (A4)$$

with $R_{in} = [(x_n-x_i)^2+(y_n-y_i)^2+(z_n-z_i)^2]^{1/2}$

which represents the distance between the control point (x_i, y_i, z_i) and the centroid of the n-th field cell (x_n, y_n, z_n), and

$$DV_n = (\xi_2 - \xi_1)\,(\eta_2 - \eta_1)\,(\zeta_2 - \zeta_1)$$

is the volume of the n-th cell, in terms of the coordinates of the grid points of the cell.

The numerical experiments show that the applicability of the far field approximation is good if $R_{in}/t > 2.5$, with

$$t = [(\xi_2 - \xi_1)^2 + (\eta_2 - \eta_1)^2 + (\zeta_2 - \zeta_1)^2]^{1/2}$$

the maximum dimension of the cell ΔV_n, i.e., the length of its diagonal.

Acknowledgement

This research is supported by the Aeronautics R&D Board, and the Aeronautical Development Agency, Government of India.

References

1. Johnson, F.T., James, R.M., Bussoletti, J.E., Woo, A.C. and Young, D.P.: A Transonic Rectangular Grid Embedded Panel Method. AIAA Paper 82-0953,1982.

2. Ravichandran, K.S., Arora, N.L. and Singh, R.: Transonic Full Potential Solutions by an Integral Equation Method. AIAA Journal, Vol. 22, No. 7, July 1984, pp. 882-888.

3. Oskam, B.: Transonic Panel Method For Full Potential Equation Applied to Multi-Component Airfoils. AIAA Journal, Vol. 23, No. 9, September 1985, pp. 1324-13 . Also AIAA paper 83-1855, 1983.

4. Erickson, L.L. and Strande, S.M.: A Theoretical Basis For Extending Surface -Panelling Methods to Trasonic Flow. AIAA Journal, Vol. 23, No. 12, Dec. 1985, pp. 1860-1867.

5. Sinclair, P.M.: A Three-dimensional Field-Integral Method for the Calculation of Transonic Flow on Complex Configurations - Theory and Preliminary Results. Aeronautical Journal, June/ July 1988, Vol. 92, pp.235-241.

6. Samant, S.S., Bussoletti, J.E., Johnson, F.T., Burkhart, R.H., Everson, B.L., Melvin, R.G., Young, D.P., Erickson, L.L., Madson, M.D. and Woo, A.C.: TRANAIR: A Computer Code for Transonic Analyses of Arbitrary Configurations. AIAA Paper 87-0034, January 1987.

7. Erickson,L.L., Madson,M.D., and Woo, A. C.: Application of the TranAir Full Potential Code to the F-16A. AIAA Journal, Vol. 24, No. 8, August 1987, pp. 540-545.

8. Kandil, O.A. and Hu, H.: Integral Equation Solution for Transonic and Subsonic Aerodynamics, in Notes on Numerical Fluid Mechanics, Vol.21, (Eds.) Ballman, J., Eppler, R. and Hackbusch, W., Vieweg 1988, pp. 101-109.

9. Kandil, O.A. and Hu, H.: Full Potential Integral Solution for Transonic Flows with and without Embedded Euler Domains. AIAA Journal, Vol. 26, No. 9, September 1988, pp. 1079-1086.

10. Samant, S.S., Bussoletti, J.E., Johnson, F.T., Melvin, R.G. and Young, D.P.: Transonic Analysis of Arbitrary Configurations using Locally Refined Grids, in Lecture Notes in Physics, Vol. 323 (Eds.) Dwoyer, D.L., Hussaini, M.Y. and Voigt, R.G., Springer Verlag 1989, pp. 518-522.

11. Baker, T.J.: Computations of Transonic Potential Flow, in Computational Methods for Turbulent, Transonic, and Viscous Flows, (Ed.) J.A. Essar, Hemisphere Pub. 1983, pp. 213-289.

12. Holst, T.L.: Fast, Conservative Algorithm for solving the Transonic Full Potential Equation. AIAA Journal Vol. 18, No. 12, Dec. 1980, pp. 1431-1439.

13. Osher, S., Hafez, M. and Whitlow, W. Jr.: Entropy Condition Satisfying Approximations for the Full Potential Equation of Transonic Flow. Mathematics of Computation, Vol. 44, No. 169, Jan. 1985, pp. 1-29.

14. Morino, L., Chen. L.T., and Suciu, E.O.: Steady and Oscillatory Subsonic and Supersonic Aerodynamics around Complex Configurations. AIAA Journal, Vol. 13, March 1975, pp. 368-374.

15. Johnson, F.T.: A General Method for the Analysis and Design of Arbitrary Configurations in Incompressible Flows. NASA CR 3079, 1980.

16. Salmond, Deborah, J.: A Cell-vertex Multigrid Scheme for solution of the Euler Equations for Transonic Flow Past a Wing. Lecture Notes in Physics, Vol. 264, Springer-Verlag 1986, pp.549-553.

17. Bailey,F.R. and Ballhaus,W.F.: Comparison of Computed and Experimental Pressures for Transonic Flows about Isolated Wings and Wing-Fuselage Configurations. NASA SP-347, pp. 1213-1231, 1975.

18. Sacher, P.: Numerical Solutions for Three-Dimensional Cases -Swept Wings, Sec. 7 in `Test Cases for Inviscid Field Methods'. AGARD-AR-211, 1985.